

新型远红外 Ge-Ga-Te-CsCl 硫系玻璃的光学特性

程 辞, 王训四*, 徐铁峰, 祝清德, 孙礼红, 廖方兴, 潘章豪, 刘 硕, 戴世勋, 沈 祥

(宁波大学高等技术研究院红外材料及器件实验室, 浙江 宁波 315211)

摘 要: 利用传统的熔融-淬冷法制备了一系列新型的掺杂卤化物 CsCl 的 Te 基玻璃。通过差示扫描量热仪和 Fourier 红外光谱仪等测试了玻璃样品的热学及光学性能。结果表明, 该玻璃具有良好的热学及光学性质。 $(\text{Ge}_{15}\text{Ga}_{10}\text{Te}_{75})_{80}(\text{CsCl})_{20}$ 玻璃样品的析晶温度 T_x 和转变温度 T_g 的差值 ΔT 最大, 达到了 118 °C。随着 CsCl 含量的增加, 玻璃的密度随之减小, 但是吸收截止边先发生蓝移然后再向长波方向移动, 其原因在于玻璃的结构及其均匀性的改变。此外, 光学带隙的最大值仅为 0.721 eV。通过提纯消除了 Ge-Ga-Te-CsCl 玻璃中杂质的影响, 并且提纯后的玻璃在 2~20 μm 波长范围内有着平坦的红外光学窗口。

关键词: 碲基玻璃; 吸收截止边; 光学带隙; 远红外

中图分类号: TQ171.1; TQ171.73 文献标志码: A 文章编号: 0454-5648(2016)01-0136-06

网络出版时间: 2015-12-23 17:19:59

网络出版地址: <http://www.cnki.net/kcms/detail/11.2310.TQ.20151223.1719.021.html>

Optical Characteristics of Novel Ge-Ga-Te-CsCl Far-infrared Chalcogenide Glasses

CHENG Ci, WANG Xunsi*, XU Tiefeng, ZHU Qingde, SUN Lihong, LIAO Fangxing, PAN Zhanghao, LIU Shuo,
DAI Shixun, SHEN Xiang

(Laboratory of Infrared Material and Devices, The Research Institute of Advanced Technologies, Ningbo University,
Ningbo 315211, Zhejiang, China)

Abstract: To develop new glass materials for bio-sensing and far infrared applications, a series of novel tellurium glasses doped with halide CsCl were prepared and investigated by traditional melt-quenching method. Thermal and optical parameters of glass samples were measured by differential scanning calorimetry (DSC) and Fourier transforming infrared spectroscopy (FTIR), etc. Experiment results indicate these glasses have good thermal and optical properties. The highest value of ΔT (the difference between the glass onset crystallization temperature T_x and the glass transition temperature T_g) reaches up to 118 °C corresponding to $(\text{Ge}_{15}\text{Ga}_{10}\text{Te}_{75})_{80}(\text{CsCl})_{20}$ glass composition. With the increase of CsCl, the density reduces gradually, but the absorption edge has a blue shift first and then shifts to a long-wavelength region. The reasons lie in the changes of glass structure and its homogeneity. In addition, the largest value of optical band gap is only 0.721 eV. With a purifying process, the affections of impurities in Ge-Ga-Te-CsCl chalcogenide glasses can be eliminated effectively and the purified glasses have a flat infrared optical window between 2 and 20 μm , which imply that these glasses are well candidate for the applications of far infrared optic imaging and sensing.

Keywords: tellurium glasses; absorption edge; optical band gap; far infrared

收稿日期: 2000-07-04。 修订日期: 2000-08-13。

基金项目: 国家自然科学基金(61435009, 61177087, 61377099); 国家 973 计划(2012CB722703); 国家科技部重大国际合作(2011DFA12040); 浙江省教育厅科研基金(R1101263); 宁波市自然科学基金(610118); 宁波大学王宽诚幸福基金; 宁波大学优秀学位论文培育基金(PY2014014)

第一作者: 程 辞(1989—), 男, 硕士研究生。

通信作者: 王训四(1979—), 男, 副研究员。

Received date: 2000-07-04. Revised date: 2000-08-13.

First author: Cheng Ci (1989—), male, Master.

E-mail: chengci1990@163.com

Correspondent author: Wang Xunsi (1979—), male, associate professor, Ph.D. degree.

E-mail: xunsiwang@siom.ac.cn

1 Introduction

In recent decades, far infrared detections have attracted unprecedented attention particularly in the finding of exo-planet life^[1-11]. The Darwin mission, conducted by European Space Agency, with a purpose of exploring the existence of life in outer space is the most impressive. CO₂, one of the critical molecules to synthetic organic life, is the primary objective to detect.

Due to its excellent properties such as outstanding infrared transparency, lower phonon energy, high linear and nonlinear refractive index^[12-15], chalcogenide glasses are considered to be ideal materials for infrared applications. However, the main absorption band of CO₂ locates at 15 μm, therefore, S- or Se- based chalcogenide glasses can't match with far infrared(FIR) application because the infrared cut-off wavelengths of S- and Se-based glasses are only up to 8 μm and 11 μm, respectively^[16-17]. To meet the requirement of FIR transparency window, it seems inevitable to develop Te-based glasses. Wilhelm *et al.*^[7] explored out that Ge-Te-I glass system possesses a wide infrared transparency window with a cut-off wavelength beyond 25 μm. But I₂ is prone to volatilization during the evacuation and fiber fabrication. Adon *et al.*^[18] reported that Ge-As-Te glass system has favorable glass formability and stable structure. However, the element of As is pernicious to our environment. Danto *et al.*^[6] revealed that element Ga doping into Ge-Te binary glass system can improve thermal stability and infrared transmission remarkably. Nevertheless, a noticeable absorption band around 15–20 μm can not be eliminated. Recently, Wang *et al.*^[19-20] proposed that halides, acting as a modifier added into Te- based glass, could decrease the formation of tellurium micro-crystals. Moreover, halogen with high electro-negativity and Cs⁺ with low polarizability makes the width of the forbidden band broader in the glass network. Furthermore, halides are harder to volatilize than halogen. Up to now, comprehensive research or report about the influence of alkali halide CsCl on the structure and properties of Te-based chalcogenide glasses is scarcely to be reported.

In this study, a series of Ge-Ga-Te-CsCl chalcogenide glasses were prepared and an extensive investigation was developed to study the effect of CsCl on Ge-Ga-Te glass matrix. The thermal and optical properties were discussed by the means of DSC and FTIR analyses.

2 Experimental

Conventional melt-quenching method was adopted to prepare a series of Ge-Ga-Te-CsCl chalcogenide glass samples. The raw materials Ge, Ga, Te with 5N purity and CsCl (3N) were weighed accurately and transferred into quartz ampoules that were then sealed under vacuum at a pressure of 1×10^{-3} Pa. The sealed ampoules were

placed in rocking furnaces and were heated at 850 °C for 15 h to homogenize the mixtures. Then, the ampoules were quenched in ice water and annealed at 10 °C below T_g in preheated furnaces. After that, the glass rods were taken out from ampoules and were cut into discs. Finally, the round glass discs were polished for testing.

The Archimedes' principle was used to determine the density by DH-300M (the accuracy is ± 0.001 g/cm³). X-ray powder diffraction (XRD) analysis by Germany Bruker D2 using Cu K_α radiation and scanning electron microscopy (SEM) were performed to determine the crystalline or amorphous state of samples. Differential scanning calorimetry (DSC) was carried out to confirm T_g (glass transition temperature) and T_x (onset temperature of glass crystallization) in the temperature range from 50 to 350 °C at a heating rate of 10 °C/min by a thermal analyze (TAQ 2000). The visible to near infrared transmission spectra in the range of 400–2 500 nm were acquired from a spectrophotometer (Perkin-Elmer Lambda 950). The IR transparency windows were obtained using Fourier transforming infrared spectroscopy (Nicolet 380) in the range of 4000–400 cm⁻¹. The Raman spectra were recorded in the range of 80–800 cm⁻¹ using a Raman scattering spectroscopy (Renishaw In Via) with an Ar⁺ ion laser. The spectral resolution was set to 1 cm⁻¹. All optical tests were performed at room temperature.

3 Results and Discussions

3.1 XRD analysis

A series of (Ge₁₅Ga₁₀Te₇₅)_{100-x}(CsCl)_x glass samples were successfully prepared for $x=0, 3, 5, 7, 10, 15,$ and 20. All glass samples are black and opaque in the visible region. To confirm the amorphous nature of these glass samples, XRD analysis were conducted. The XRD patterns are shown in Fig. 1. The results show that all curves are smooth and peaks are diffusive, no sharp peaks exist in the patterns. Hence, the well amorphous nature of these glass samples could be verified.

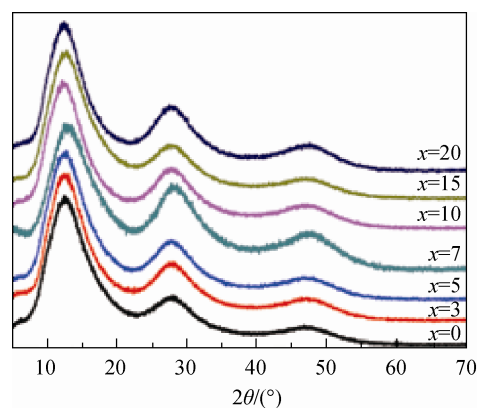


Fig. 1 XRD patterns of (Ge₁₅Ga₁₀Te₇₅)_{100-x}(CsCl)_x glass samples

3.2 Physical properties

The components and physical parameters of glass samples are listed in Table 1. With the increase of CsCl, the density ρ decreased from 5.735 g/cm³ to 5.447 g/cm³ while the molar volume increased gradually as shown in Fig. 2. Density is usually determined by the elemental relative atomic mass and the packing efficiency of atoms^[21]. The relative atomic mass of CsCl is 168, smaller than that of GeTe₄ (585) and GaTe₃ (454). Thus, CsCl has a small polarization rate that results in the lower packing efficiency of atoms. The GeTe₄ and GaTe₃ units were reduced with the increase of CsCl. Thus, the density ρ decreased along with the increase of CsCl. The relationships between molar volume and density can be described by the following formula (1).

$$V_m = \frac{\sum M_i}{\rho} = \frac{\sum A_i \times B_i}{\rho} \quad (1)$$

Where, M_i is the molar mass of glass sample, A_i is the molar concentration, B_i is the molecular weight of the component, ρ is the density of glass sample.

Table 1 Physical properties of (Ge₁₅Ga₁₀Te₇₅)_{100-x}(CsCl)_x glass samples

Mole fraction x /%	Thickness d /cm	Density ρ /(g·cm ⁻³)	Mole volume V_m /(cm ³ ·mol ⁻¹)
0	0.180	5.735	19.869
3	0.116	5.503	21.002
5	0.122	5.491	21.244
7	0.133	5.487	21.457
10	0.150	5.479	21.784
15	0.156	5.468	22.322
20	0.138	5.447	22.904

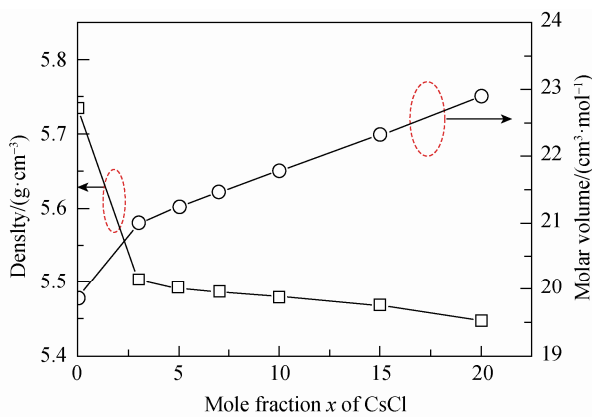


Fig. 2 Density and molar volume of glass samples versus the content of CsCl

3.3 Thermal properties

The thermal properties of Ge–Ga–Te–CsCl glass samples were investigated by DSC instrument. Figure 3 shows the DSC curves of glass samples. The difference ΔT between T_x and T_g is always used to evaluate the

thermal stability of glasses. The higher value of ΔT indicates the stronger ability against crystallization. The values of T_g , T_x and ΔT for the glass samples are listed in Table 2. Obviously, the ΔT increases with the increase of CsCl. It is believed that chlorine atoms traps metallic electrons from tellurium, and forms the covalent bonds between Te and Cl atoms. As a result, the tendency of tellurium correlated to the formation of microcrystal was controlled. Therefore, the thermal stability of Ge–Ga–Te–CsCl glass samples improved. The largest value of ΔT was 118 °C, corresponding to the composition $x=20$ which possesses superior thermal properties than other glass samples. In contrast to base glass composition Ge₁₅Ga₁₀Te₇₅, the ΔT value of (Ge₁₅Ga₁₀Te₇₅)₈₀(CsCl)₂₀ glass is 6 °C greater. Further, the ΔT of all glass samples are above 111 °C. It indicates that CsCl improves thermal characteristics of the base glass composition Ge₁₅Ga₁₀Te₇₅.

Table 2 Thermal properties of Ge–Ga–Te–CsCl glass samples

x	T_g /°C	T_x /°C	ΔT /°C
0	172	284	112
3	172	284	112
5	173	286	113
7	169	283	114
10	170	286	116
15	167	284	117
20	167	285	118

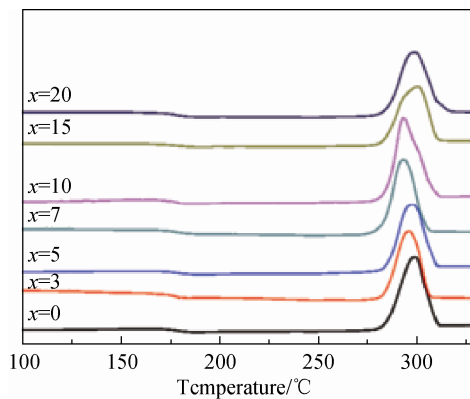


Fig. 3 DSC curves of Ge–Ga–Te–CsCl glass samples

3.4 Raman spectra analysis

The structure representation of a glass could be obtained through Raman spectra. The Raman spectra of the glass samples are presented in Fig. 4. Three strong vibration bands appear around 65, 130, and 156 cm⁻¹, respectively. A broad and low intensity vibration band appears around 220 cm⁻¹. The vibration bands usually result from some bonds or atomic group. The first and second vibration bands are attributed to Ge–Te bonds while the peak at 155 cm⁻¹ is ascribed to the vibration of Te–Te bonds^[22–23]. The last vibration band is assigned to

the Ge-Ge bonds^[24]. All the results show that no other structure unit appears.

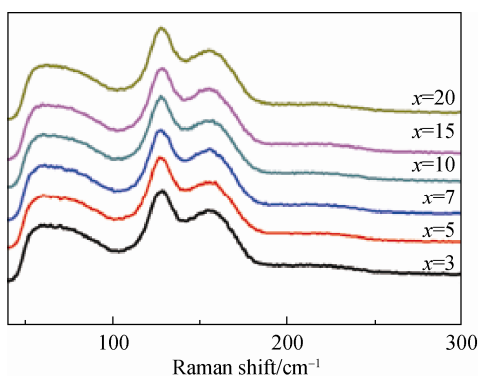


Fig. 4 Raman spectra of Ge-Ga-Te-CsCl glass samples

3.5 Structure analysis with SEM

In order to show more details in the glasses, SEM were applied to observe the surface and microstructure of glasses. Fig. 5 and Fig. 6 are the SEM images of Ge-Ga-Te-CsCl glass samples. Here, we just list two typical SEM patterns for two kinds of glasses: $(\text{Ge}_{15}\text{Ga}_{10}\text{Te}_{75})_{93}(\text{CsCl})_7$ and $(\text{Ge}_{15}\text{Ga}_{10}\text{Te}_{75})_{80}(\text{CsCl})_{20}$, which stand for the normal and abnormal glasses separately. In Fig. 5, the surfaces of the glass samples were nearly the same when x ranged from 0 to 7. However, some holes like gas bubbles could be observed when x ranged from 10 to 20, just shown as Fig. 6.

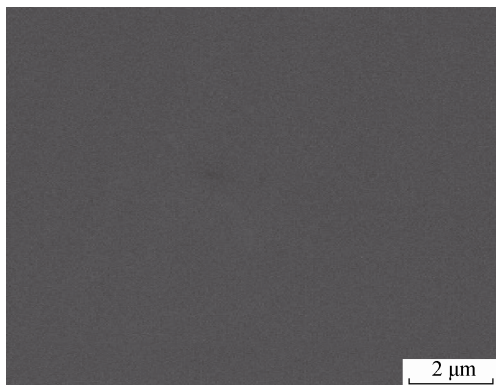


Fig. 5 SEM image for the glass sample $(\text{Ge}_{15}\text{Ga}_{10}\text{Te}_{75})_{93}(\text{CsCl})_7$

The diameters of these holes range from 0.76 to 0.93 μm , and their perimeters (2.386 4–2.920 2 μm) fit well with the mid-infrared light. According to the scattering optics, the Mie scattering can be adopted to explain the subsequent appearances as that the scattering intensity I_{scat} is inversely square relations to the wavelength of incident light^[25].

$$I_{\text{scat}} = k \frac{1}{\lambda^2} \quad (2)$$

Where, k is a coefficient correlated with glass thickness and incident angle, etc. λ is the wavelength of incident light.

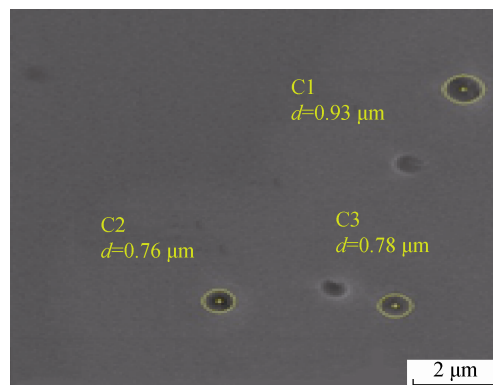


Fig. 6 SEM image for the glass sample $(\text{Ge}_{15}\text{Ga}_{10}\text{Te}_{75})_{80}(\text{CsCl})_{20}$

According to the Lambert-Beer law^[26], the scattering absorbance A_{scat} can be defined as:

$$A_{\text{scat}} = \lg(I_{\text{in}}/I_{\text{scat}}) = \lg(1/T) \quad (3)$$

Where, T is the light transmittance, and then,

$$T = 10^{-k\lambda^{-2}} \quad (4)$$

3.6 Near infrared absorption spectra and optical band gap analysis

The near infrared absorption spectra of glass samples are shown in Fig. 7. With the increase of CsCl, the optical absorption edge shifted to a shorter-wavelength region first and then turned into a longer-wavelength region. Eventually, the absorption cut-off wavelength ranges from 1 703 to 1 788 nm as listed in Table 3. The reason to account for the normal blue shift may be the addition of CsCl. With the content of high electronegativity of chlorine atoms and low polarizability of Cs^+ increasing, the width of forbidden band became broader gradually. Consequently, the absorption cut-off edge had a normal blue shift. The reason for the abnormal red shift on the absorption cut-off edge can be explained with the scattering loss of the glass holes. From

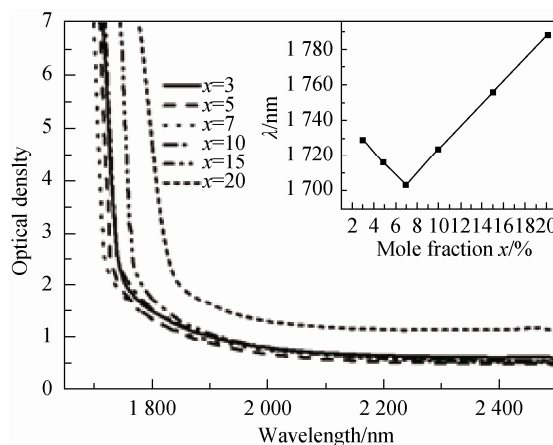


Fig. 7 Near infrared absorption spectra of Ge-Ga-Te-CsCl glass samples.

Insert figure shows the relationships between absorption edge and CsCl content.

equation (2), the shorter the wavelength of light is, the stronger the scattering intensity is. And this results in an abnormal red shift of the absorption cut-off edge.

The relationship between the absorption coefficient $\alpha(\omega)$ and the optical band-gap E_{opt} is given by the Tauc law^[27]:

$$\alpha(\omega) \cdot \hbar\omega = B(\hbar\omega - E_{opt})^m, \tag{5}$$

where E_{opt} is the Tauc optical band gap, $\alpha(\omega)$ is the absorption coefficient determined by $\alpha = 2.303 A/d$ (A is optical density, d is thickness of glass sample), \hbar is the Plank constant, ω is the angular frequency of incident light, m is a parameter depending on the transition type of absorption edge. For amorphous materials, the allowed direct transition are corresponding to $m = 1/2$. B is a constant that depends on the width of the localized states in the band gap, which can be calculated by the following equation:

$$B = \frac{(4\pi/c)\sigma_0}{n_0\Delta E}, \tag{6}$$

Where σ_0 is the electrical conductivity under absolute zero, n_0 is the static refractive index, c is the speed of the light in vacuum, ΔE is the width of the located-state tail. The direct band gap is shown in illustration of Fig. 8 and the values are listed in Table 3. Here, the tendency of direct band gap is opposite to that of the absorption cut-off edge.

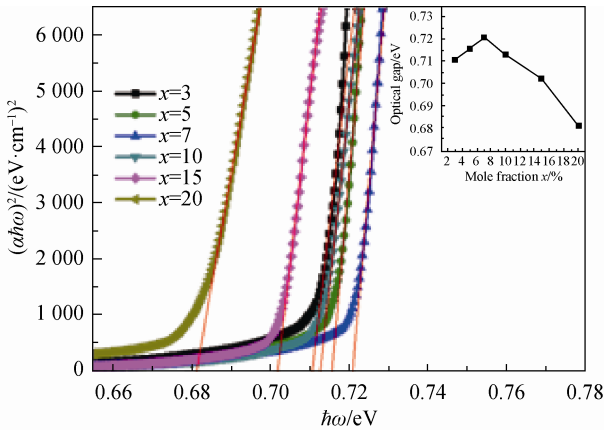


Fig. 8 The relationship between $(\alpha \cdot \hbar\omega)^2$ and $\hbar\omega$ for glass samples

The insert figure shows the relationships between the direct band gap and CsCl content

Table 3 Cut-off wavelengths λ and direct band gap E_{opt} of Ge–Ga–Te–CsCl glass samples

x	λ/nm	E_{opt}/eV
3	1 729	0.711
5	1 716	0.716
7	1 703	0.721
10	1 724	0.713
15	1 756	0.702
20	1 788	0.681

3.7 Infrared spectra analysis

Figure 9 presents the infrared transmission spectra of Ge-Ga-Te-CsCl glasses. With equations (2), (3) and (4), the transmission under scattering can be figured out for compare, as that also shown in Fig. 9. Here, infrared cut-off wavelengths of these glass samples were all beyond 20 μm . However, when x was above 10, the infrared spectra of these glasses had a slope between 2.5–14 μm . This abnormal characteristic may be attributed to the little holes in these glasses and their transmission ratios are affected by the scattering loss. Meanwhile, some absorption peaks occurred in the transmission spectra. The first absorption peak which locates at 9.8 μm is attributed to the effect of Si–O bonds^[19]. The absorption band between 15–20 μm may be ascribed to Ge–O or Ga–O bonds^[28–29]. These absorption peaks are mainly produced by oxide impurities from raw materials. Therefore, to eliminate the effect of impurities, raw materials have to be purified. $(\text{Ge}_{15}\text{Ga}_{10}\text{Te}_{75})_{95}(\text{CsCl})_5$ glass sample was chosen for purification. The method was to distill Te with 400×10^{-6} Mg into the ampoule which contained other raw materials under vacuum. The following steps were the same as the original method. The infrared spectrum of purified glass is seen in Fig. 10. Compared to unpurified glass sample, no obvious absorption peak appears in the infrared spectrum of purified glass. And the purified glass exhibits a wide and flat optical transmitting window.

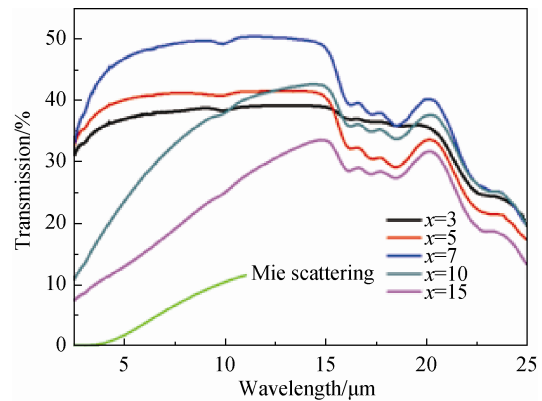


Fig. 9 Infrared transmission spectra of glass samples

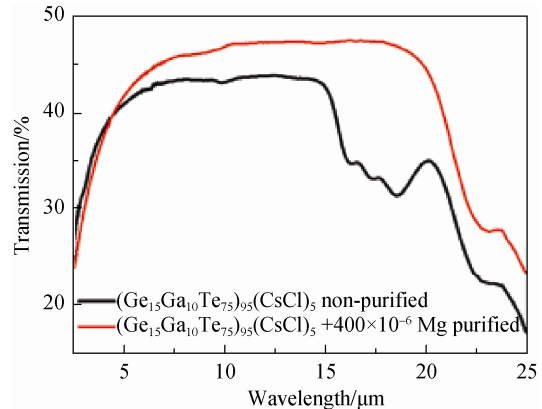


Fig. 10 Infrared spectra of $(\text{Ge}_{15}\text{Ga}_{10}\text{Te}_{75})_{95}(\text{CsCl})_5$ glasses

4 Conclusions

Novel Ge-Ga-Te-CsCl glasses were prepared and investigated. The results indicate that the glass samples have favorable thermal stability. The thermal stability of $(\text{Ge}_{15}\text{Ga}_{10}\text{Te}_{75})_{80}(\text{CsCl})_{20}$ glass sample with the highest ΔT values (118 °C) is superior to other glass samples. The largest value of optical band gap is 0.721 eV. From the infrared spectra, these glasses have wide optical windows with the cut-off wavelength beyond 25 μm .

References:

- [1] ZHANG X H, FONTENEAU G, LUCAS J. Tellurium halide glasses. New materials for transmission in the 8–12 μm range[J]. *J Non-Cryst Solids*, 1988, 104(1): 38–44.
- [2] LUCAS J, ZHANG X H. The tellurium halide glasses[J]. *J Non-Cryst Solids*, 1990, 125(1): 1–16.
- [3] KANAMORI T, TERUNUMA Y, TAKAHASHI S, et al. Chalcogenide glass fibers for mid-infrared transmission[J]. *Lightwave Technology*, 1984, 2(5): 607–613.
- [4] QUÉMARD C, SMEKTALA F, COUDERC V, et al. Chalcogenide glasses with high non linear optical properties for telecommunications[J]. *J Phys Chem Solids*, 2001, 62(8): 1435–1440.
- [5] BUREAU B, ZHANG X H, SMEKTALA F, et al. Recent advances in chalcogenide glasses[J]. *J Non-Cryst Solids*, 2004, 345(1): 276–283.
- [6] DANTO S, HOUZOT P, BOUSSARD - PLEDEL C, et al. A Family of far-infrared-transmitting glasses in the Ga-Ge-Te system for space applications[J]. *Adv Funct Mater*, 2006, 16(14): 1847–1852.
- [7] WILHELM A A, BOUSSARD - PLEDEL C, COULOMBIER Q, et al. Development of far-infrared-transmitting te based glasses suitable for carbon dioxide detection and space optics[J]. *Adv Mater*, 2007, 19(22): 3796–3800.
- [8] MAURUGEON S, BUREAU B, BOUSSARD-PLEDEL C, et al. Te-rich Ge-Te-Se glass for the CO₂ infrared detection at 15 μm [J]. *J Non-Cryst Solids*, 2009, 355(37): 2074–2078.
- [9] CONSEIL C, BASTIEN J C, BOUSSARD-PLEDEL C, et al. Te-based chalcogenide glasses for far-infrared optical fiber[J]. *Opt Mater Express*, 2012, 2(11): 1470–1477.
- [10] ZAKERY A, ELLIOTT S R. Optical properties and applications of chalcogenide glasses: a review[J]. *J Non-Cryst Solids*, 2003, 330(1): 1–12.
- [11] CUI S, BOUSSARD-PLEDEL C, LUCAS J, et al. Te-based glass fiber for far-infrared biochemical sensing up to 16 μm [J]. *Opt Express*, 2014, 22(18): 21253–21262.
- [12] BAHISHTI A A, KHAN M A M, PATEL B S, et al. Effect of laser irradiation on thermal and optical properties of selenium-tellurium alloy[J]. *J Non-Cryst Solids*, 2009, 355(45): 2314–2317.
- [13] HE Y J, WANG X S, NIE Q H, et al. Glass formation and optical properties of Ge-Te-Ga-CuI far-IR transmitting chalcogenide glasses[J]. *Infrared Phys Techn*, 2013, 60(1): 129–133.
- [14] PAMUKCHIEVA V, SZEKERES A, TODOROVA K, et al. Evaluation of basic physical parameters of quaternary Ge-Sb-(S, Te) chalcogenide glasses[J]. *J Non-Cryst Solids*, 2009, 355(50): 2485–2490.
- [15] 尹冬梅, 顾朝晖, 陈祎, 等. $((\text{GeSe}_2)(\text{SnSe}_2)_{0.5})_{100-x}\text{Te}_x$ 系统硫系玻璃的光学性能及结构[J]. *硅酸盐学报*. 2014, 42(7): 945–950
YIN D M, GU Z, CHEN Y, et al. *J Chin Ceram Soc*, 2014, 42(7): 945–950.
- [16] TROLES J, NIU Y, DUVERGER-ARFUSO C, et al. Synthesis and characterization of chalcogenide glasses from the system Ga-Ge-Sb-S and preparation of a single-mode fiber at 1.55 μm [J]. *Mater Res Bull*, 2008, 43(4): 976–982.
- [17] ZHANG X H, MA H, LUCAS J. Evaluation of glass fibers from the Ga-Ge-Sb-Se system for infrared applications[J]. *Opt Mater*, 2004, 25(1): 85–89.
- [18] ALDON L, LIPPENS P E, OLIVIER-FOURCADE J, et al. Thermal stability of some glassy compositions of the Ge-As-Te ternary[J]. *Chalcogenide Letters*, 2010, 7(1): 187–196.
- [19] WANG X S, NIE Q H, WANG G X, et al. Investigations of Ge-Te-AgI chalcogenide glass for far-infrared application[J]. *Spectrochim Acta A*, 2012, 86(1): 586–589.
- [20] XU H J, WANG X S, NIE Q, et al. Glass formation and properties of Ge-Ga-Te-ZnI₂ far infrared chalcogenide glasses[J]. *J Non-Cryst Solids*, 2014, 383(1): 212–215.
- [21] EL-SAYED S M, SAAD H M, AMIN G A, et al. Physical evolution in network glasses of the Ag-As-Te system[J]. *J Phys Chem Solids*, 2007, 68(5): 1040–1045.
- [22] KOLOBOV A V, FONS P, TOMINAGA J, et al. Crystallization-induced short-range order changes in amorphous GeTe[J]. *J Phys Condens Matter*, 2004, 16(44): S5103.
- [23] SEN S, GJERSING E L, AITKEN B G. Physical properties of $\text{Ge}_x\text{As}_{2x}\text{Te}_{100-3x}$ glasses and Raman spectroscopic analysis of their short-range structure[J]. *J Non-Cryst Solids*, 2010, 356(41): 2083–2088.
- [24] FUKUNAGA T, TANAKA Y, MURASE K. Glass formation and vibrational properties in the (Ge, Sn) system[J]. *Solid State Comm*, 1982, 42(7): 513–516.
- [25] GOMPFF B, PECHA R. Mie scattering from a sonoluminescing bubble with high spatial and temporal resolution[J]. *Phys Rev E*, 2000, 61(5): 5253.
- [26] ZACCANTI G, BRUSCAGLIONI P. Deviation from the Lambert-Beer law in the transmittance of a light beam through diffusing media: experimental results[J]. *J Modern Opt*, 1988, 35(2): 229–242.
- [27] TAUC J. *Amorphous and liquid semiconductors*[M]. Plenum: Springer Science & Business Media, 1974: 88–90.
- [28] ZHANG S, ZHANG X, BARILLOT M, et al. Purification of $\text{Te}_{75}\text{Ga}_{10}\text{Ge}_{15}$ glass for far infrared transmitting optics for space application[J]. *Opt Mater*, 2010, 32(9): 1055–1059.
- [29] WANG G, NIE Q, BARJ M, et al. Compositional dependence of the optical properties of novel Ge-Ga-Te-CsI far infrared transmitting chalcogenide glasses system[J]. *J Phys Chem Solids*, 2011, 72(1): 5–9.